

# Nonlinear Modeling and Control of Human Heart Rate Response During Exercise With Various Work Load Intensities

Teddy M. Cheng\*, *Member, IEEE*, Andrey V. Savkin, *Senior Member, IEEE*, Branko G. Celler, *Member, IEEE*, Steven W. Su, *Member, IEEE*, and Lu Wang

**Abstract**—The first objective of this paper is to introduce a nonlinear system to model the heart rate (HR) response during and after treadmill walking exercise. The model is a feedback interconnected system that has components to describe the central and peripheral local responses to exercise and their interactions. The parameters of the model were experimentally identified from subjects walking on a treadmill at different speeds. The stability of the obtained nonlinear model was mathematically proven. The modeling results demonstrate that the proposed model can be useful in examining the cardiovascular response to exercise. Based on the nonlinear model, the second objective is to present a computer-controlled treadmill system for the regulation of HR during treadmill exercise. The proposed nonlinear controller consists of feedforward and feedback components. The designed control system was experimentally verified and the results demonstrated that the proposed computer-controlled treadmill system regulated the HR of the experimental subjects according to two different exercising HR profiles, indicating that it can play an important role in the design of exercise protocols for individuals.

**Index Terms**—Cardiovascular system, exercise, H-infinity control, linear-quadratic (LQ) control, modeling, nonlinear systems, parameter estimation.

## I. INTRODUCTION

**D**URING dynamic exercise, the cardiovascular system increases the delivery of blood and oxygen to working muscles as the metabolic demand increases, resulting in an increase in heart rate (HR) and stroke volume. Obtaining a model that describes the cardiovascular system during exercise could improve our understanding of exercise physiology. Understanding the aetiology of HR response during, and recovery after an exercise, may also be beneficial to predicting and reducing cardiovascular disease mortality [1], [2]. This may also lead to an

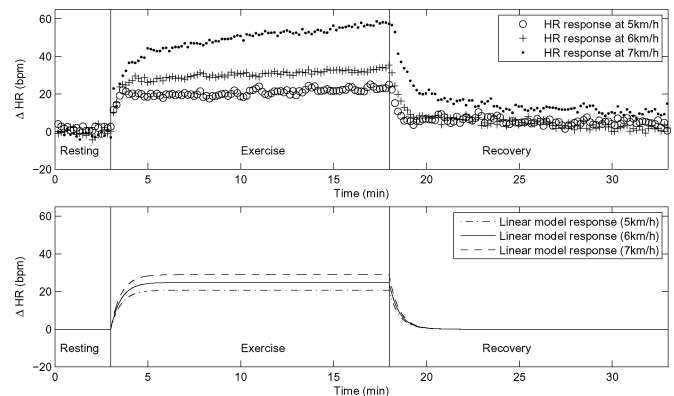


Fig. 1. (Top) Typical HR responses to walking exercise with speed: 5 km/h (circle), 6 km/h (plus), and 7 km/h (dot). (Bottom) Step responses of a stable first-order linear system with speed: 5 km/h (dashed-dotted), 6 km/h (solid), and 7 km/h (dashed).

improvement in developing training protocols for athletics and more efficient weight loss protocols for the obese and in facilitating assessment of physical fitness and health of individuals [3]. Furthermore, knowing the cardiovascular system responses to the stress induced by the physical exercise provides us another perspective on how this system functions. For instance, these models may provide some useful measures for the prevention of cardiac failure from dialysis.

Studying and modeling of HR response during exercise have been carried out by a number of researchers [4]–[9]. Brodan *et al.* [4] and Hajek *et al.* [5] modeled the HR response, both during exercise and recovery phases. Their models consist of feedforward and feedback components [10] and are reliable for short-duration exercises but are not sufficient for explaining responses to long-duration exercise. As shown in [6]–[8], the HR will continue to increase during prolonged exercise, possibly due to factors such as increases in body temperature, dehydration, and accumulation of metabolites. The exercising HR response was modeled in [9] by a Hammerstein system, a system that consists of a static nonlinearity cascaded at the input of a linear system. Again, their models were derived for describing HR responses for short-duration exercise. Besides modeling, they also studied the control and regulation of the HR response during exercise.

A major challenge in modeling physiological systems is that they exhibit nonlinear behaviors. The HR response to exercise is of no exception. Fig. 1 shows typical human HR responses to

Manuscript received January 24, 2008; revised March 29, 2008. First published June 10, 2008; current version published October 31, 2008. This work was supported by the Australian Research Council. Asterisk indicates corresponding author.

\*T. M. Cheng is with the School of Electrical Engineering and Telecommunications, The University of New South Wales, Sydney, NSW 2052, Australia (e-mail: t.cheng@ieec.org).

A. V. Savkin is with the School of Electrical Engineering and Telecommunications, The University of New South Wales, Sydney, NSW 2052, Australia.

B. G. Celler is with the School of Electrical Engineering and Telecommunications, The University of New South Wales, Sydney, NSW 2052, Australia, and also with TeleMedCare Pty. Ltd., Rosebery, NSW 2018, Australia.

S. W. Su is with the Faculty of Engineering, University of Technology, Sydney, NSW 2007, Australia.

L. Wang was with the School of Electrical Engineering and Telecommunications, The University of New South Wales, Sydney, NSW 2052, Australia. She is now with Cochlear Ltd., Lane Cove, NSW 2066, Australia.

Digital Object Identifier 10.1109/TBME.2008.2001131

walking exercises. There are at least two nonlinear phenomena that can be observed from Fig. 1. First, the increase in HR does not behave linearly, i.e., the increase in HR is not proportional to the walking speed [9], [11]–[13], and it may be due to the nonlinear increase in metabolic demand [13].

Second, at a high walking speed, the HR response shows a slowly increasing behavior that resembles the cardiovascular drift phenomenon [6]–[8]. The drift phenomenon is more prominent in high-intensity exercises than in low-intensity exercises. From a modeling point of view, the drift phenomenon can be described by a step response of a stable system, but with a very long transient behavior. On the other hand, the transient behavior seems to last much shorter in the case with a slow walking speed. Such a change in transient behavior may explain the nonuniform shape of the HR responses, as shown in Fig. 1. It seems that the dynamics of the HR response vary as the walking speed increases. In fact, a similar phenomenon was also observed in muscle blood flow at the onset of dynamic exercise [10], [14]. In other words, the transient behavior of HR responses depends on the walking speed or the intensity of the exercise. This is in contrast to typical step responses of a stable linear time-invariant system; the transient behavior of the linear system is invariant with respect to the magnitude of the input. For example, the time constant of step responses of a stable first-order time-invariant linear system is the same no matter what the magnitudes of the inputs are (see Fig. 1).

The ability to control the HR during exercise is of importance in the design of exercise protocols for patients with cardiovascular diseases and in developing rehabilitation exercises to aid patients recovering from cardiothoracic surgery. The control of HR response during exercise has been reported in [9], [15], and [16]. Among them, a number of different control strategies or algorithms have been successfully applied, e.g., classical PID control [15],  $H_\infty$  control [9], and model reference control [16]. The models studied in [15] and [16] were linear, and the control designs were carried out simply using linear control techniques. Linear control was also adopted for the Hammerstein system considered in [9], as the input nonlinearity in a Hammerstein system can be easily canceled, reducing it to a linear control problem. However, as mentioned before, the HR responses to exercise exhibit nonlinear phenomena and these phenomena may become especially significant for patients with cardiovascular diseases or recovering after cardiosurgery. Hence, linear control techniques cannot be applied in such circumstances. Therefore, we will investigate and explore the usefulness of modern nonlinear control algorithms and techniques for the control of the HR response.

The present paper had two main purposes. First, a nonlinear model was proposed to describe the HR response to treadmill walking exercise. The exercising HR response was modeled from the central and the local responses perspective. The advantage of this approach was that the model could provide us with a platform to examine the interactions between the central and local responses. Also, it may describe the HR response over a longer exercise duration. The stability property of the model was also proven in a mathematically rigorous way. Using the model, the second aim of this paper was to design and imple-

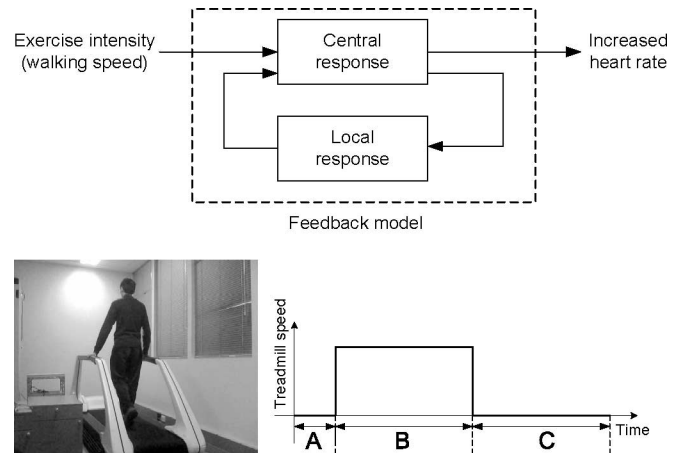


Fig. 2. (Top) Feedback representation of the proposed HR model. (Bottom) Walking exercise with treadmill speed profile for system identification. (A) Resting. (B) Exercise. (C) Recovery periods.

ment a computer-controlled treadmill system for the control of HR kinetics. Since the HR model is nonlinear, the controller was designed using a novel approach utilizing the techniques of controlling so-called hybrid dynamical systems that are being actively studied in the control engineering community (see, e.g., [17], [18], and references therein). The resulting controller consists of feedforward and feedback components that provide better performance without trading off robustness. Finally, the computer-controlled treadmill system was experimentally validated and its performance was demonstrated via experimental applications.

## II. PROBLEM DESCRIPTION

The modeling problem was the development and identification of a nonlinear state-space model that describes the HR response of an exerciser during and after a treadmill walking exercise. The input to the model is the intensity of the exercise, in particular, the speed of the treadmill. The output of the model is the HR of the exerciser. The schematic of the model is shown in Fig. 2. The parameters of the model were identified from the step responses of HR of different experimental subjects, as shown in Fig. 2. The distinctive feature of our approach to identifying the parameters was that we reformulated it as a parameter estimation problem of a multi-input multi-output (MIMO) dynamical systems. Specifically, a set of model parameters was estimated by *simultaneously* utilizing all the HR responses of different subjects to various step inputs. This approach allows us to obtain a subject-independent model that could reasonably describe the HR responses of any exerciser to various treadmill speeds. This is important if a controller needs to be designed to accommodate a range of individuals of varying levels of cardiovascular fitness.

The control problem considered in this paper involves the design and implementation of a nonlinear controller based on the proposed nonlinear HR model. The job of the controller is to control and regulate an exerciser's HR according to a given exercising HR profile. The controller takes the measured HR and

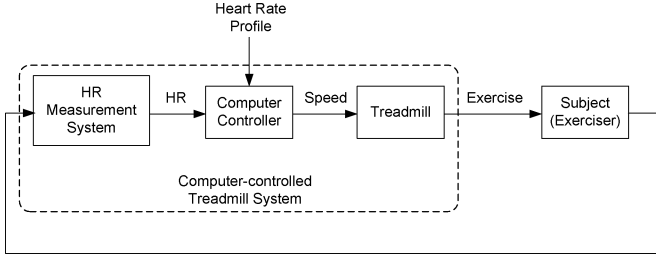


Fig. 3. Computer-controlled treadmill system.

a desired exercise HR profile as its inputs, whereas its output is an actuating signal that controls the speed of the treadmill. The controller was then implemented on a computer and integrated with an electric treadmill, forming a fully automated, computer-controlled treadmill system for walking exercise. The block diagram of the computer-controlled treadmill system is shown in Fig. 3.

### III. MODEL

We first introduce the following nonlinear state-space control system to model the behavior of HR response to treadmill walking exercise:

$$\begin{aligned} \dot{x}_1(t) &= -a_1 x_1(t) + a_2 x_2(t) + a_2 u^2(t) \\ \dot{x}_2(t) &= -a_3 x_2(t) + \phi(z(t)) \\ z(t) &= x_1(t), \quad \phi(z(t)) := \frac{a_4 x_1(t)}{1 + \exp(-(x_1(t) - a_5))} \end{aligned} \quad (1)$$

where  $x(0) = [x_1(0) \ x_2(0)]' = [0 \ 0]'$  is the initial condition and  $a_1, \dots, a_5$  are positive scalars. The output  $z(t)$  relates to the change of HR from rest and the control input  $u(t)$  describes the speed of the treadmill. System (1) can be viewed as a feedback interconnected system (see Fig. 2). The component  $x_1(t)$  may describe the change of HR mainly due to the central response to exercise, whereas the component  $x_2(t)$  may describe the slower and more complex local peripheral effects. In terms of the central response,  $x_1$  may be used to model both the parasympathetic and the sympathetic neural inputs [6]. The component  $x_2$  could be utilized to describe the complex slow-acting effects from, for example, the hormonal systems, the peripheral local metabolism, the increase in body temperature, and the loss of body fluid due to sweating and hyperventilation [7], [8], [19]. For instance, in the case of the peripheral local metabolism, the accumulated metabolic byproducts, such as adenosine,  $K^+$ ,  $H^+$ ,  $PO_4^{3-}$ , lactic acid, and other metabolites, cause vasodilation and hyperaemia in active muscles [10]. Vasodilation in the active muscles causes a reduction in total peripheral resistance that, in turn, causes a decrease in the mean arterial blood pressure. In order to regulate the blood pressure, the cardiac output needs to be increased, meaning that stroke volume and HR are increased via the baroreceptor reflex [12]. So, the positive feedback signal  $x_2$ , or a dynamic disturbance input to the  $x_1$  subsystem, may be treated as a reaction to the effects from the peripheral local responses or factors. In this case, the metabo-

lites from the peripheral local metabolism further accelerate the HR during exercise [12].

The nonlinear function  $\phi(x_1)$  has the property that  $\phi(x_1) \approx 0$  when  $x_1$  is small; whereas, when  $x_1$  is much larger than  $a_5$ ,  $\phi(x_1)$  approaches the linear function  $a_4 x_1$  [in fact,  $a_4/(1 + \exp(-(x_1 - a_5)))$  is a sigmoidal function]. If  $x_1$  is small and  $a_5$  is large, the variable  $x_1$  is multiplied by a small factor [i.e.,  $a_4/(1 + \exp(-(x_1 - a_5))) \approx 0$ ] in the second equation of (1), so  $x_2$  becomes nearly independent of  $x_1$ . If  $x_1(0) = x_2(0) = 0$  and the input  $u(t)$  is small, the state  $x_1(t)$  may not be large enough to make the factor  $a_4/(1 + \exp(-(x_1(t) - a_5)))$  become significant, and  $x_2(t)$  will remain approximately 0. As a result, system (1) can be approximated by the system  $\dot{x}_1(t) = -a_1 x_1(t) + a_2 u^2(t)$  with  $x_2(t) \equiv 0$ . On the other hand, if the input  $u(t)$  is sufficiently large, the state  $x_1(t)$  will be driven to a level that the factor  $a_4/(1 + \exp(-(x_1(t) - a_5)))$  is significant, and  $x_2(t)$  is no longer independent of  $x_1(t)$ . Therefore, the dynamics of the model become more complex as the magnitude of the input increases. Here, we hypothesize that the local peripheral effects [i.e.,  $x_2(t)$ ] become relatively more significant when the change of HR [i.e.,  $x_1(t)$ ] is large. In fact, previous studies showed that as the intensity of exercise increases, a more complex model is needed to describe the muscle blood flow at the onset of exercise [10], [14].

In system (1), the input  $u(t)$  (i.e., the speed of treadmill or the exercise intensity) drives the system nonlinearly (quadratically), describing the nonlinear increase of HR in response to an increase in walking speed. It has been observed that there is a curvilinear relationship between aerobic demand and walking speed [11], [12]. In fact, the increase in metabolic cost from walking on a level terrain is approximately proportional to the square of walking speed [13].

#### A. Experimental Setup for System Identification

The parameters in system (1) were identified from experimental data. The setup of the experiment is described next.

1) *Subjects*: Six healthy male subjects were studied. The group of subjects ( $n = 6$ ) had a mean age 29.3 years (standard deviation = 5.9 years, range 23–38 years), a mean weight 68.5 kg (standard deviation = 12.6 kg, range 53–85 kg), a mean height 174 cm (standard deviation = 3.4 cm, range 169–178 cm), and a mean body mass index (BMI) 22.5 kg/m<sup>2</sup> (standard deviation = 3.4 kg/m<sup>2</sup>, range 18–27 kg/m<sup>2</sup>). Written informed consent was obtained from all participants, and the study was approved by the Human Research Ethics Advisory panel (Panel D) of the University of New South Wales.

2) *Procedure*: Each subject completed three walking exercise sessions in separate occasions (see Fig. 2). In each session, the subject was requested to walk on a treadmill at a given speed (5, 6, and 7 km/h) for 15 min with a recovery period of 15 min. The HR of the subject was recorded from 3 min before the exercise until 15 min after the cessation of the walking exercise. The period before the exercise and the 15-min period after the exercise are called the resting and recovery periods, respectively. Fig. 2 shows the speed profile of treadmill at three different

periods. During both the resting and the recovery periods, the subject was requested to maintain a standing posture.

3) *Data Acquisition and Preprocessing*: In this paper, a fully motorized medical grade treadmill (Powerjog) was used. The HR was monitored by the commonly used wireless Polar system (Polar Electro, Inc.) and recorded by LabVIEW (National Instruments). The HR data were first filtered using the moving average with a 5-s window and then sampled at a 10-s period. Since the proposed system (1) is to model the change of HR from rest, the resting HR for each subject was estimated from the 3-min resting period before a walking exercise. The mean resting HR of all six subjects was 74 beats/min (bpm) [standard deviation (SD) = 8.4] and denoted by  $HR_{rest}$ .

### B. Parameter Estimation

A set of parameters  $\{a_1, a_2, \dots, a_5\}$  in system (1) was identified from the HR responses of all subjects. In other words, using HR responses of all subjects, a common model was identified. From the experiment, three sets of input–output measurements of HR (where the input is the speed of the treadmill and the output is the HR) were recorded for each subject, meaning that 18 sets of input–output HR measurements (six subjects  $\times$  three exercise sessions per subject) were collected. We then estimated the parameters using the 18 sets of input–output data *simultaneously*. Therefore, we considered it as a parameter estimation problem of the following MIMO system, i.e., a system with 18 sets of input–output measurements:

$$\dot{\mathbf{x}}(t) = \mathbf{f}(\mathbf{x}(t), \mathbf{a}, \mathbf{u}(t)), \quad \mathbf{z}(t) = \mathbf{C}\mathbf{x}(t), \quad \mathbf{x}(0) = \mathbf{0} \quad (2)$$

where  $\mathbf{C} \in \mathbb{R}^{18 \times 36}$  is the measurement matrix,  $\mathbf{x} := [\mathbf{x}_1 \ \mathbf{x}_2 \ \dots \ \mathbf{x}_{18}]' \in \mathbb{R}^{36}$ ,  $\mathbf{a} := [a_1 \ a_2 \ \dots \ a_5]' \in \mathbb{R}^5$ ,  $\mathbf{u} := [u_1 \ u_2 \ \dots \ u_{18}]' \in \mathbb{R}^{18}$ , and  $\mathbf{z} = [z_1 \ z_2 \ \dots \ z_{18}]' \in \mathbb{R}^{18}$ . For  $i = 1, 2, \dots, 18$ , the vector  $\mathbf{x}_i := [x_{i,1} \ x_{i,2}]' \in \mathbb{R}^2$  and the scalar  $z_i \in \mathbb{R}$  are the state vector and the output from the input  $u_i$ , respectively. The elements of the measurement matrix  $\mathbf{C}$  are defined as

$$C_{i,j} = \begin{cases} 1, & \text{if } j = 2i - 1 \\ 0, & \text{otherwise} \end{cases}$$

for  $i = 1, 2, \dots, 18$  and  $j = 1, 2, \dots, 36$ . For practical reasons and computational efficiency, the unit of time  $t$  in system (2) was defined in minutes and some scaling were also carried out for the control input and the output. **As for the control input, the speed of the treadmill was normalized by 8 km/h (since we assumed the maximum walking speed is 8 km/h).**

We let  $\mathcal{S}$  be a set consisting of the integers 0, 5, 6, and 7. Then, the normalized input vector  $\mathbf{u}$  in (2) was defined as

$$\mathbf{u}(t) := \frac{[s_1(t) \ s_2(t) \ \dots \ s_{18}(t)]'}{8} \quad (3)$$

where  $s_i(t)$ ,  $i = 1, 2, \dots, 18$ , is the actual speed of treadmill in kilometers per hour and  $s_i(t) \in \mathcal{S}$ , since three treadmill speeds (namely 5, 6, and 7 km/h) were used in the experiment. Including 0 km/h in the set  $\mathcal{S}$  reflects that HR measured during recovery period was also considered in the parameter estimation process. For  $i = 1, 2, \dots, 18$ , the output  $z_i(t)$  from the input  $u_i(t)$  was

TABLE I  
ESTIMATED PARAMETER  $\hat{a}$  AND PARAMETER VARIATION  $\delta\hat{a}$  [CONFIDENCE INTERVAL =  $(\hat{a} - \delta\hat{a}, \hat{a} + \delta\hat{a})$ ]

Parameter estimates, $\hat{a}$ ( $\delta\hat{a}$ )				
$\hat{a}_1$	$\hat{a}_2$	$\hat{a}_3$	$\hat{a}_4$	$\hat{a}_5$
1.84 (0.36)	24.32 (4.36)	$6.36 \times 10^{-2}$ ( $1.95 \times 10^{-2}$ )	$3.21 \times 10^{-3}$ ( $6.84 \times 10^{-4}$ )	8.32 (0.44)

defined as

$$z_i(t) := \frac{HR_i(t) - 74}{4} \quad (4)$$

where  $HR_i(t)$  is the absolute HR at time  $t$ , 74 bpm is the mean resting HR of all subjects, and 4 is the scaling factor. In other words, for  $i = 1, 2, \dots, 18$ ,  $z_i(t)$  is the scaled change of HR from the mean resting HR due to the input  $u_i(t)$ . By considering the MIMO system (2), the Levenberg–Marquardt method [20] was then employed for the parameter estimation of the vector  $\mathbf{a}$ . Based on the linear approximate method [21], an approximate  $100(1 - \alpha)\%$  independent confidence interval for each parameter estimate was also determined and it is given by  $(\hat{a}_i - \delta\hat{a}_i, \hat{a}_i + \delta\hat{a}_i)$ , for  $i = 1, 2, \dots, 5$ , where  $\hat{a}_i$  denotes the estimate of parameter  $a_i$  obtained from the Levenberg–Marquardt method. In this paper, an  $\alpha$  level of 0.05 was used for obtaining the confidence intervals of the parameter estimates and for all other significant tests. Table I shows the estimated parameters and their confidence intervals.

### C. Model Selection and Validation

In this section, two issues are to be addressed: 1) comparing the proposed model with another candidate model and 2) statistically validating the proposed model consisting of the estimated parameters. As for the model selection or comparison is concerned, it is interesting to investigate the benefits of using the proposed model (1) when comparing with a simple linear model. Since the proposed model (1) is a second-order nonlinear system, it is reasonable to compare it with a second-order linear system. In fact, when  $\phi(x_1) = a_4 x_1$  and  $v = u^2$ , the proposed model (1) reduces to a second-order linear system with input  $v$ . Therefore, by setting  $v = u^2$ , we have two candidate models: 1) a nonlinear model (1) with parameters  $\{a_1, a_2, \dots, a_5\}$  and 2) a linear model with parameters  $\{a_1, a_2, \dots, a_4\}$  and  $\phi(x_1) = a_4 x_1$ . The two completing models were compared based on the Akaike information criterion (AIC) and the F ratio test methods [22]. The parameters  $\{a_1, a_2, \dots, a_4\}$  of the linear system were estimated using the procedure presented in Section III-B [ $\hat{a}_1 = 2.0$  ( $\delta\hat{a}_1 = 0.47$ ),  $\hat{a}_2 = 25.12$  ( $\delta\hat{a}_2 = 5.15$ ),  $\hat{a}_3 = 0.097$  ( $\delta\hat{a}_3 = 0.034$ ),  $\hat{a}_4 = 0.0032$  ( $\delta\hat{a}_4 = 0.0012$ )]. The AIC of the nonlinear model (1) was found to be smaller than that of the linear counterpart. Also, the F ratio test (with  $\alpha = 0.05$ ) showed that the extra parameter  $a_5$  in the nonlinear model provided a significant improvement when comparing with the linear system, and hence, the inclusion of this parameter in the nonlinear model (1) was

justified, meaning that the nonlinear system (1) is a better model than the second-order linear model.

Based on the nonlinear regression method, the identified model (1) was then validated by comparing the recorded HR data and the predicted responses from the model at three different treadmill speeds. The HR data used for model validation here were the same as those collected for parameter estimation in Section III-B. For each treadmill speed, there were six HR responses from the subjects, and these responses were treated as replicated measurements. Then, an F-test based on the analysis of variance (ANOVA) was adopted [23] to check the fit of the model at treadmill speeds, namely 5, 6, and 7 km/h. For each speed, the test statistics were less than the critical value at the significant level  $\alpha = 0.05$ , indicating that the model is adequate.

#### D. Stability Analysis

System (1) represents a feedback interconnected nonlinear system. Its stability has to be examined since it would be of little practical interest if the system is unstable, for instance, it is obvious that the response of HR to a finite-intensity exercise should not approach infinity. Even though system (1) is nonlinear, its stability can be examined by a simple mean. System (1) is first rewritten into the following form:

$$\dot{x}(t) = \mathcal{A}x(t) + \mathcal{B}_1\bar{\phi}(z(t)) + \mathcal{B}_2u^2(t), \quad z(t) = Cx(t) \quad (5)$$

where  $x(t) = [x_1(t) \ x_2(t)]'$ ,  $\bar{\phi}(z(t)) := \phi(z(t))/a_4$ , and

$$\mathcal{A} := \begin{bmatrix} -a_1 & a_2 \\ 0 & -a_3 \end{bmatrix}, \quad \mathcal{B}_1 := \begin{bmatrix} 0 \\ a_4 \end{bmatrix},$$

$$\mathcal{B}_2 := \begin{bmatrix} a_2 \\ 0 \end{bmatrix}, \quad C := \begin{bmatrix} 1 \\ 0 \end{bmatrix}'.$$

Then, the following proposition provides a way for checking the stability of system (5).

**Proposition 3.1:** Suppose that there exists a symmetric positive definite matrix  $P = P' > 0$  such that the algebraic Riccati inequality

$$\mathcal{A}'P + P\mathcal{A} + P\mathcal{B}_1\mathcal{B}_1'P + C'C < 0 \quad (6)$$

holds. Then, the system (5) is stable in the following sense: the output  $z$  of the system is bounded for any bounded input  $u$  and for any initial condition  $x_0$ .

**Proof:** The nonlinearity  $\bar{\phi}(z)$  satisfies the cone-bounded condition:  $|\bar{\phi}(z)| \leq |z|$  for all  $z \in \mathbb{R}$ . Therefore, if there exists a solution  $P = P' > 0$  to the algebraic Riccati inequality (6), then according to the strict bounded real lemma [24], the origin  $x = 0$  of the unforced system (5) (i.e., with input  $u = 0$ ) is globally asymptotically stable. Hence, the output  $z$  of the system (5) is bounded for any bounded input  $u$ . ■

By substituting  $a = \hat{a}$  (see Table I) in system (5), there exists a symmetric positive definite matrix

$$P = \begin{bmatrix} 2.22 & -16.33 \\ -16.33 & 2946.01 \end{bmatrix}$$

such that the Riccati inequality (6) holds. Then, Proposition 3.1 implies that system (1) is input-output stable. In other words,

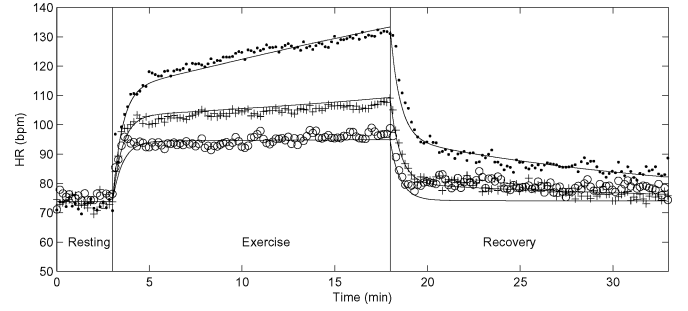


Fig. 4. Average HR responses of all six subjects ( $n = 6$ ) with treadmill speeds: 5 km/h (circle), 6 km/h (plus), and 7 km/h (dot) and simulated HR responses (solid lines) from the proposed nonlinear model.

for any bounded treadmill speed  $u$ , the output  $z$  of the model (1), i.e., the HR response, with the estimated parameter vector  $\hat{a}$  is also bounded.

Not only is the solution of system (1) bounded for any bounded input, its solution is also nonnegative for all  $t \geq 0$  and for any control input  $u(\cdot)$  and any nonnegative initial condition  $x_1(0) \geq 0$ ,  $x_2(0) \geq 0$ . This is stated in the following proposition.

**Proposition 3.2:** Consider system (1) with strictly positive parameters  $a_1, a_2, \dots, a_5 > 0$ . Suppose that the initial condition satisfies  $x_1(0) \geq 0$  and  $x_2(0) \geq 0$ . Then, the solution  $x_1(t)$ ,  $x_2(t)$  of system (1) satisfies  $x_1(t) \geq 0$  and  $x_2(t) \geq 0$  for all  $t \geq 0$  and for all input  $u(\cdot)$ .

**Proof:** If  $x_1(t) = 0$  and  $x_2(t) \geq 0$  and either  $x_2(t) > 0$  or  $u(t) \neq 0$ , then using (1),  $\dot{x}_1(t) > 0$ . Similarly, if  $x_2(t) = 0$  and  $x_1(t) > 0$ , then  $\dot{x}_2(t) > 0$ . When  $u(\cdot) \equiv 0$  and  $x_1(0) = x_2(0) = 0$ , the solution  $x_1(t)$ ,  $x_2(t)$  is at the equilibrium  $x_1(\cdot) \equiv x_2(\cdot) \equiv 0$ . If we let  $\mathcal{F}$  be the set  $\{(x_1, x_2) \in \mathbb{R}^2 : x_1 \geq 0 \text{ and } x_2 \geq 0\}$ , then the set  $\mathcal{F}$  with system (1) is an invariant set, meaning that a solution starting in  $\mathcal{F}$  remains in  $\mathcal{F}$  for all  $t \geq 0$ . ■

#### E. Identified Model

By combining (1), (3), and (4) with the estimated parameters in Table I, we obtained a nonlinear model that describes the HR (bpm) during and after treadmill exercise, and it is given as follows:

$$\begin{aligned} \dot{x}_1(t) &= -1.84x_1(t) + 24.32x_2(t) + 0.38s^2(t) \\ \dot{x}_2(t) &= -6.36 \times 10^{-2}x_2(t) + \phi(x_1(t)) \\ \text{HR}(t) &= 4.0x_1(t) + \text{HR}_{\text{rest}} \\ \phi(x_1(t)) &:= \frac{3.21 \times 10^{-3}x_1(t)}{1 + \exp(-(x_1(t) - 8.32))} \end{aligned} \quad (7)$$

where  $\text{HR}_{\text{rest}} = 74$  bpm,  $x_1(0) = x_2(0) = 0$ ,  $s(t)$  is the speed of treadmill in kilometers per hour, the unit of time  $t$  is in minutes, and  $\text{HR}(t)$  is in bpm. The simulated HR responses using the nonlinear model (7) together with the average responses of all the subjects at different treadmill speeds are shown in Fig. 4. The nonlinear model (7) overall fits well into the average responses of all the intensities. Note that the shape of the HR

response generated from the nonlinear model changes as the speed of the treadmill increases, and this cannot be simply explained by linear systems. This also explains a benefit of using a nonlinear model over a linear model for describing exercise HR response [14].

#### IV. CONTROLLER DESIGN

The objective of this section is to present a control design for the nonlinear system (7) obtained from the last section, aiming to control and regulate the HR of an exerciser during treadmill exercise by varying the speed of the treadmill. In other words, the speed of the treadmill  $s(t)$  is the control input, whereas the HR( $t$ ) is the controlled variable. Our design is based on approximating the obtained nonlinear model by a piecewise linear system. The proposed nonlinear controller is based on switching between a set of “basic controllers” that are defined in various subregions of the system state–space. To design these “basic controllers,” we employ the powerful techniques of linear-quadratic (LQ) and  $H^\infty$  control. The designed nonlinear system belongs to the class of hybrid dynamical systems that have been extensively studied in the modern control literature in recent years (see, e.g., [17] and [18]).

##### A. Nonlinear Control System

With proper scaling (since scaling makes model analysis and controller design easier), system (7) is written in a state–space form as follows:

$$\dot{\eta}(t) = A\eta(t) + B_1\Phi(\eta_1(t)) + B_2g(u(t)), \quad y(t) = C\eta(t) \quad (8)$$

where

$$A = \begin{bmatrix} -3.07 \times 10^{-2} & 2.7 \times 10^{-2} \\ 0 & -1.06 \times 10^{-3} \end{bmatrix}, \quad g(u(t)) := u^2(t)$$

$$\eta = \begin{bmatrix} \eta_1 \\ \eta_2 \end{bmatrix}, \quad B_1 = \begin{bmatrix} 0 \\ 1 \end{bmatrix}, \quad B_2 = \begin{bmatrix} 2.7 \times 10^{-2} \\ 0 \end{bmatrix}, \quad C = \begin{bmatrix} 1 \\ 0 \end{bmatrix}'$$

$$\Phi(\eta_1(t)) := \frac{8.03 \times 10^{-4}\eta_1(t)}{1 + \exp(-15(\eta_1(t) - 5.55 \times 10^{-1}))}.$$

To obtain (8), we have defined a normalized output  $y(t) = \eta_1(t) := x_1(t)/15$  [i.e.,  $y(t) := (\text{HR}(t) - \text{HR}_{\text{rest}})/60$ ] and a normalized input  $u(t) := s(t)/8$ . Also, for the ease of controller design analysis, the time unit of  $t$  in (8) is in seconds, instead of minutes as in (7). System (8) is a nonlinear system with nonlinearity  $\Phi(\eta_1)$  and nonlinear control input  $g(u)$ . To overcome the control input nonlinearity, a transformed input  $v(t) = g(u(t))$  is defined, whereas the function  $\Phi(\eta_1)$ , as shown in Fig. 5, can be approximated by a piecewise linear function

$$\gamma(\eta_1) = \begin{cases} 0, & \text{if } \eta_1 \leq 0.419 \\ 1.52 \times 10^{-3}\eta_1 - 6.34 \times 10^{-4}, & \text{if } \eta_1 > 0.419. \end{cases}$$

In fact,  $\gamma(\eta_1)$  is obtained by linearizing the function  $\Phi(\eta_1)$  at  $\eta_1 = 0$  and  $0.5$ . As a result, system (8) can be approximated by a piecewise affine system [25]. In this paper, we adopted the technique of controlling hybrid dynamical systems to design a two degrees-of-freedom controller that consists of a piecewise

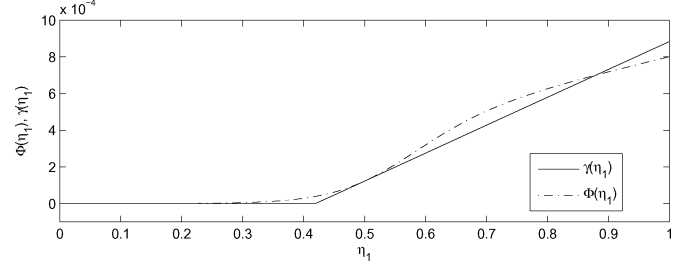


Fig. 5. Approximation of nonlinear function  $\Phi(\eta_1)$  by a piecewise linear function  $\gamma(\eta_1)$ .

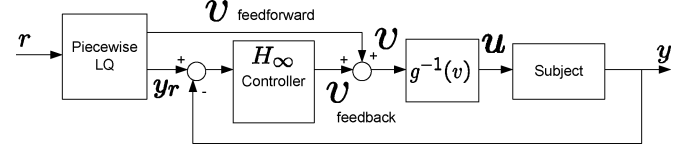


Fig. 6. Control configuration with feedforward and feedback controllers.

LQ feedforward and a  $H^\infty$  feedback controllers, as shown in Fig. 6, for the control and regulation of HR responses.

##### B. LQ Feedforward Controller Design

First, a feedforward controller was designed using the piecewise LQ optimal control technique of [25]. In doing so, we also incorporated an integral action in the controller.

Define two partitions of the state–space:

$$X_1 := \{[\eta_1 \ \eta_2]' \in \mathbb{R}^2 \mid \eta_1 < 0.419\}$$

$$X_2 := \{[\eta_1 \ \eta_2]' \in \mathbb{R}^2 \mid \eta_1 \geq 0.419\}.$$

Next, define

$$\bar{A}_i = \begin{bmatrix} A_i & 0_{2 \times 1} & a_i \\ -C & 0 & 0 \\ 0_{1 \times 2} & 0 & 0 \end{bmatrix}, \quad \bar{B} = \begin{bmatrix} B_2 \\ 0 \\ 0 \end{bmatrix}, \quad \bar{\eta}(t) = \begin{bmatrix} \eta(t) \\ e(t) \\ 1 \end{bmatrix}$$

for  $\eta \in X_i$  and  $i = 1, 2$ , where

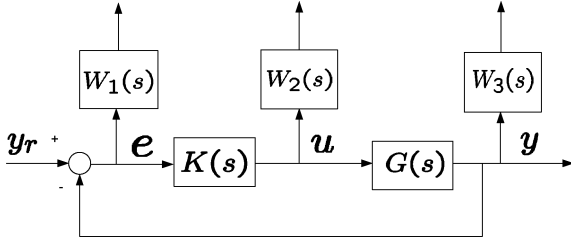
$$A_1 = \begin{bmatrix} -3.07 \times 10^{-2} & 2.7 \times 10^{-2} \\ 0 & -1.06 \times 10^{-3} \end{bmatrix}$$

$$A_2 = \begin{bmatrix} -3.07 \times 10^{-2} & 2.7 \times 10^{-2} \\ 1.52 \times 10^{-3} & -1.06 \times 10^{-3} \end{bmatrix}$$

$e(t) = \int_0^t (r - C\eta(t))dt$ ,  $a_1 = [0 \ 0]'$ ,  $a_2 = [0 \ -6.39 \times 10^{-4}]'$ , and  $r$  is the constant reference input. Therefore, we have  $\dot{\bar{\eta}}(t) = \bar{A}_i\bar{\eta}(t) + \bar{B}v(t)$ ,  $y(t) = \bar{C}\bar{\eta}(t)$ , for  $\eta \in X_i$  where  $\bar{C} = [C \ 0 \ 0]$ . Then, the control problem is to minimize the cost function  $J = \int_0^\infty (\bar{\eta}'(t)\bar{Q}\bar{\eta}(t) + v'(t)Rv(t))dt$ , for any given  $\bar{Q} \geq 0$  and  $R > 0$ . In the control design, the value of  $R$  was chosen as  $R = 350$ , and the matrix  $\bar{Q}$  was chosen as a positive semidefinite diagonal matrix  $\bar{Q} = \text{diag}(\{0, 0, 0.5, 0\})$  with elements  $\{0, 0, 0.5, 0\}$  on the diagonal. The minimizing control law is

$$v(t) = L_i\bar{\eta}(t), \quad \eta \in X_i, \quad i = 1, 2 \quad (9)$$

where  $L_1 = [-0.88 \ -0.97 \ 0.038 \ 0]$  and  $L_2 = [-0.91 \ -1.0 \ 0.038 \ 0.019]$ . The gains  $L_1$  and  $L_2$

Fig. 7.  $H_\infty$  mixed sensitivity control problem.

(9) were computed by using PWLTool, a MATLAB toolbox for piecewise linear systems [26]. Hence, the LQ feedforward controller is in the form

$$\begin{aligned} \dot{\bar{\eta}}(t) &= \bar{A}_i \bar{\eta}(t) + \bar{B} v(t) + B_r r, & y_r(t) &= \bar{C} \bar{\eta}(t) \\ v(t) &= L_i \bar{\eta}(t), & & \text{for } \eta \in X_i \end{aligned} \quad (10)$$

where  $\bar{\eta}(0) = [0 \ 0 \ 0 \ 1]'$ ,  $B_r = [0 \ 0 \ 1 \ 0]'$ , and  $r$  is the reference input. In other words, the input to this feedforward controller is the reference  $r$  and the output are the feedforward control  $v(t)$  and the “smoothed” reference  $y_r(t)$ . It is clear that the LQ controller is a switching controller [18], as the control law is chosen depending on the state  $\eta(t)$ .

### C. $H_\infty$ Controller Design

To cope with the uncertainty in the model, we designed a feedback controller based on the  $H_\infty$  control technique [24]. We first linearized the system (8) and then formulated the control problem as a mixed sensitivity problem [27]. Linearizing system (8) at  $\eta_0 = [0.5 \ 0.115]'$  and  $v_0 = 0.452$  results in the linearized model

$$\dot{\xi}(t) = A_2 \xi(t) + B_2 w(t), \quad \zeta(t) = C \xi(t) \quad (11)$$

where  $\xi(t) = \eta(t) - \eta_0$  and  $w(t) = v(t) - v_0$ . The transfer function of the linearized model is

$$G(s) = \frac{0.027s + 2.86 \times 10^{-5}}{s^2 + 0.0317s - 8.65 \times 10^{-6}}. \quad (12)$$

In a mixed sensitivity problem, the idea is to choose some weighing functions, namely  $W_1(s)$ ,  $W_2(s)$ , and  $W_3(s)$  to reflect the control objectives (see Fig. 7). The functions  $W_1(s)$  and  $W_3(s)$  are the sensitivity and complementary weighting functions, respectively. In general practice,  $W_1(s)$  is chosen to meet the performance specification,  $W_3(s)$  is chosen to characterize the modeling errors (multiplicative uncertainty), whereas the weighing function  $W_2(s)$  can be used to impose some restrictions on the actuator signal and/or to model an additive uncertainty. The weighing functions in this paper were chosen as

$$\begin{aligned} W_1(s) &= \frac{0.1(s + 0.083)}{(s + 8.33 \times 10^{-5})}, & W_2(s) &= \frac{70(s + 6.25 \times 10^{-4})}{(s + 4.38)} \\ W_3(s) &= \frac{100(s + 0.066)}{(s + 8.33)}. \end{aligned}$$

The weighing function  $W_1(s)$  was chosen as a high-gain low-pass filter approximating an integral action to ensure good

tracking accuracy. A first-order high-pass filter was chosen for  $W_2(s)$  to limit the controller bandwidth and magnitude. The weighing function  $W_3(s)$  was chosen so that the design allows up to  $\approx 80\%$  multiplicative modeling error and/or  $\approx 10$  s of time delay in the system. By using MATLAB Robust Control Toolbox, we obtained a robust feedback controller

$$\begin{aligned} K(s) &= \frac{8.91 \times 10^{-3}s^4 + 0.11s^3 + 0.33s^2 + 0.01s + 2.6 \times 10^{-6}}{s^5 + 9.1s^4 + 6.43s^3 + 0.42s^2 + 4.61 \times 10^{-4}s + 3.56 \times 10^{-8}} \end{aligned} \quad (13)$$

and  $\gamma = 0.9$  so that  $|S(j\omega)| \leq \gamma/|W_1(j\omega)|$ ,  $|T(j\omega)| \leq \gamma/|W_3(j\omega)|$ , and  $|K(j\omega)S(j\omega)| \leq \gamma/|W_2(j\omega)|$  for all  $\omega \in \mathbb{R}$ . The functions  $S$  and  $T$  are the sensitivity and the complementary sensitivity functions, respectively.

### V. COMPUTER-CONTROLLED TREADMILL SYSTEM

By using the control design presented in Section IV, a computer-controlled treadmill system was implemented for the regulation of HR, and its configuration is shown in Fig. 3. The system consists of three main components: a treadmill, an HR measurement system, and a computer controller.

As in Section III-A3, a fully motorized treadmill (Powerjog) was used. Here, it was connected to the computer controller via an RS232 serial port. The HR measurement system was similar to the one used for the identification of the model in Section III-A3, except that here the computer (LabVIEW) collected HR signal from the wireless Polar system every 6 s. Also, since a reliable real-time HR signal was required for the computer controller, an exponentially weighed moving average filter (exponential smoothing [28]), with filter coefficient  $\alpha = 0.75$ , was employed online. The computer controller was implemented in LabVIEW. The feedforward controller (10) was precomputed offline, whereas the robust feedback controller (13) was discretized using the zero-order hold method with a sampling period  $T = 6$  s. Then, the control signal was sent to the treadmill via the serial port.

To validate the computer-controlled treadmill system, two groups totalling of nine subjects were requested to exercise on the treadmill. The first group consists of six subjects who had preformed exercises for system identification in Section II-A1, and this group is called model development group. The second group of subjects is called control validation group. This validation group has three subjects: two males and one female, and they were not involved in either system identification or controller design. Written informed consent was obtained from all participants, and the study was approved by the Human Research Ethics Advisory panel (Panel D) of the University of New South Wales.

The control validation group was employed to test the robustness of the computer-controlled treadmill system. Each subject in both groups performed walking exercises on the treadmill and was prescribed with two sets of predefined exercise HR profiles. The goal was to control and regulate the subject's HR according to the profile. The predefined HR profiles may be viewed as

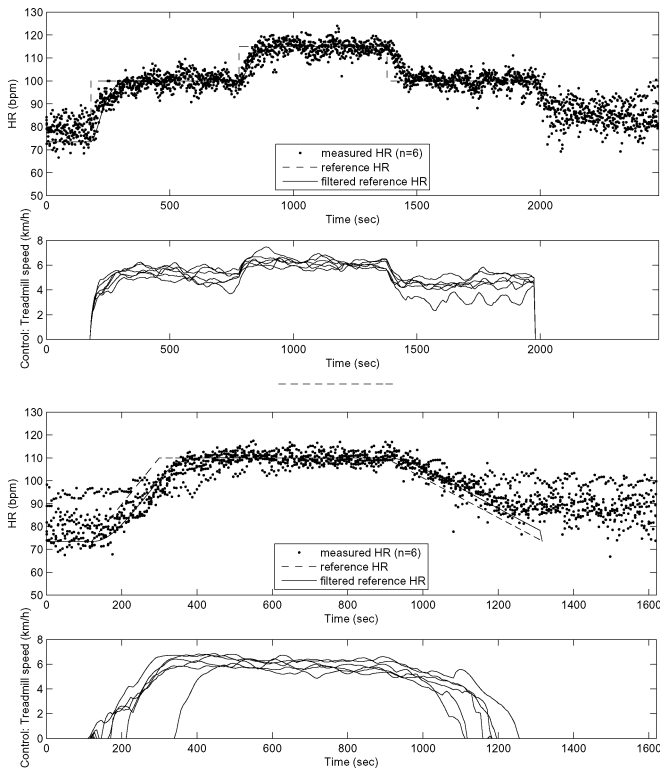


Fig. 8. (Top) First HR profile: regulation of HR at 100 and 115 bpm for the model development group ( $n = 6$ ) with the corresponding treadmill speed. (Bottom) Second HR profile: HR regulation at 110 bpm with gradually warm-up and cool-down periods for the model development group ( $n = 6$ ) with the corresponding treadmill speed.

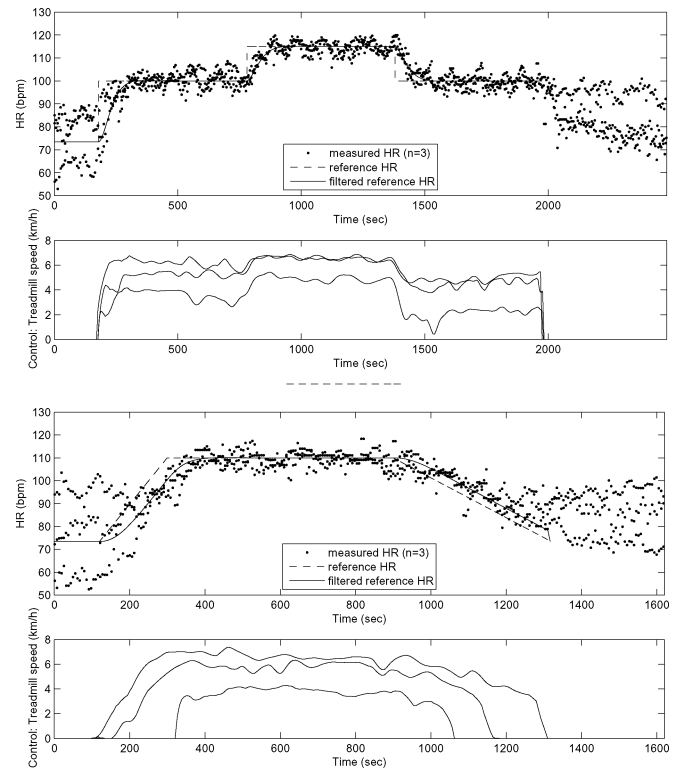


Fig. 9. (Top) First HR profile: regulation of HR at 100 and 115 bpm for the control validation group ( $n = 3$ ) with the corresponding treadmill speed. (Bottom) Second HR profile: HR regulation at 110 bpm with gradually warm-up and cool-down periods for the control validation group ( $n = 3$ ) with the corresponding treadmill speed.

some training or exercise prescriptions, since HR is commonly used as an indicator of exercise intensity [3].

The first exercise HR profile has  $3 \times 10$  min stages involving two HR levels, namely 100 and 115 bpm (representing  $\approx 51\%$ – $55\%$  and  $\approx 58\%$ – $63\%$  of maximal HR, respectively). The first 10 min stage with HR 100 bpm is considered as a warm-up period, the second 10-min stage with HR 115 bpm is the exercise period, and the last stage with HR 100 bpm is the cool-down period. Cooling down is important for preventing venous pooling after exercise and possible cardiovascular arrest for at risk individuals. The second exercise HR profile also includes the warm-up, exercise, and cool-down stages. The differences between the first and the second profiles are: 1) the warm-up period in the second exercise HR profile is 3 min long with a gradually increase of HR to 110 bpm from rest; 2) the HR level during the exercise phase is 110 bpm (representing  $\approx 56\%$ – $60\%$  of maximal HR); and 3) the cool-down period is 7 min long with HR gradually decreasing to the subjects' recovery HR from the exercise phase.

As shown in Figs. 8 and 9, the HR of each subject in both model development and control validation groups closely followed the first exercise HR profile and regulated at the predefined HR levels by using the proposed computer-controlled treadmill system. Similar results were obtained for the second exercise HR profile that are shown in Figs. 8 and 9. Therefore, the experimental results demonstrate that the proposed controller performed effectively and robustly in both the model development and control validation groups.

It is interesting to point out that some of the subjects' HR did not completely follow the second HR profile for the duration of the 7-min cool-down period (see Figs. 8 and 9). It is because the recovery HR of the subjects could not be further reduced since the treadmill already reached 0 km/h. Similarly, again in the second exercise HR profile, there was a delay before the treadmill started activating if a subject had a high resting HR, as shown in both Figs. 8 and 9. Since the subject's resting HR was higher than the reference HR, nothing could be done by the treadmill to reduce the resting HR of the subject.

By observing Figs. 8 and 9, the HR responses of the subjects indeed followed the "filtered" reference HR signals, instead of the actual reference HR signals in each exercise HR profile. Recalling from the control design in Section IV-B, the feedforward controller generates a feedforward control signal to the treadmill as well as provides a "filtered" or "smoothed" reference HR for the  $H_\infty$  feedback controller (see Fig. 6). The advantages of utilizing such a "filtered" reference HR are to improve tracking performance and to reduce control effort [27]. For the tracking of the first exercise HR profile, as shown in Figs. 8 and 9, the feedforward controller smoothed out the abrupt changes in the HR reference signals preventing overshooting in the HR responses, and allowing HR to change in a more gradual and smoother manner. This may be important, for example, in cardiac rehabilitation. However, for the tracking of the second exercise HR profile, as shown in Figs. 8 and 9, it seems that the feedforward controller not only smoothed out but also delayed the actual



HR reference. The delay was due to fact that the feedforward controller only incorporated an integral action that is good for tracking step-like references or rejecting step-like disturbances, but not for tracking ramp-like reference signals. Such a delay did not cause any problem in this study as our main concern was to regulate HR response at certain predefined levels. One could eliminate such a delay for nonstep-like references by applying the so-called internal model principle [27] and simply incorporating the reference HR signal model in the feedforward controller design.

## VI. CONCLUSION

In this paper, a nonlinear model describing the HR response to the treadmill walking exercise was proposed. The proposed model is a feedback interconnected system: consisting of a subsystem in the forward path that can be used to describe the central response and a feedback subsystem that can be utilized to describe the peripheral local responses. The model was identified from the HR responses of fit and healthy experimental subjects. Since the model is a feedback interconnected system, its stability was checked and proven in a mathematically rigorous way. The modeling results showed that the proposed model could be useful for examining the central and local responses during exercise. In fact, they showed that the HR response to walking exercise exhibits two distinct modes in terms of the speed of the response. The fast mode may describe the central response and the slow mode may reflect the peripheral local responses or factors. Also, it appears that the peripheral local response becomes more significant when the exercise intensity increases. In other words, a higher order dynamic model may be needed to explain both central and local responses simultaneously at higher intensity exercises. In fact, this agrees with the observations in [14]; as the intensity of exercise increases, a higher order dynamic model is needed for describing the muscle blood flow.

Based on this nonlinear model, a computer-controlled treadmill system was developed and implemented for the regulation of HR during treadmill exercise. The controller is nonlinear that consists of a piecewise LQ feedforward and an  $H_\infty$  feedback controllers. One of the benefits of introducing the feedforward control is to improve the performance, since robust control using  $H_\infty$  controllers is sometimes overly conservative, thus impeding performance. The computer-controlled treadmill system was experimentally validated and the results demonstrated its potential use in the design of exercise protocols for individuals.

## REFERENCES

- [1] K. P. Savonen, T. A. Laka, J. A. Laukkanen, P. M. Halonen, T. H. Rauramaa, J. T. Salonen, and R. Rauramaa, "Heart rate response during exercise test and cardiovascular mortality in middle-aged men," *Eur. Heart J.*, vol. 27, pp. 582–588, 2006.
- [2] C. R. Cole, E. H. Blackstone, F. J. Pashkow, C. E. Snader, and M. S. Lauer, "Heart rate recovery immediately after exercise as a predictor of mortality," *New England J. Med.*, vol. 341, no. 18, pp. 1351–1357, 1999.
- [3] J. Achten and A. E. Jeukendrup, "Heart rate monitoring: Applications and limitations," *Sports Med.*, vol. 33, no. 7, pp. 517–538, 2003.
- [4] V. Brodan, M. Hajek, and E. Kuhn, "An analog model of pulse rate during physical load and recovery," *Physiol. Bohemoslov.*, vol. 20, pp. 189–198, 1971.
- [5] M. Hajek, J. Potucek, and V. Brodan, "Mathematical model of heart rate regulation during exercise," *Automatica*, vol. 16, pp. 191–195, 1980.
- [6] L. B. Rowell, *Human Cardiovascular Control*. New York: Oxford Univ. Press, 1993.
- [7] J. M. Johnson and L. B. Rowell, "Forearm and skin vascular responses to prolonged exercise in man," *J. Appl. Physiol.*, vol. 39, pp. 920–924, 1975.
- [8] E. F. Coyle and G. Alonso, "Cardiovascular drift during prolonged exercise: New perspectives," *Exerc. Sports Sci. Rev.*, vol. 29, pp. 88–92, 2001.
- [9] S. W. Su, L. Wang, B. G. Celler, A. V. Savkin, and Y. Guo, "Identification and control for heart rate regulation during treadmill exercise," *IEEE Trans. Biomed. Eng.*, vol. BE-54, no. 7, pp. 1238–1246, Jul. 2007.
- [10] R. L. Hughson, "Regulation of blood flow at the onset of exercise by feed forward and feedback mechanisms," *Can. J. Appl. Physiol.*, vol. 28, no. 5, pp. 774–787, 2003.
- [11] P. E. Martin and D. J. Sanderson, "Biomechanics of walking and running," in *Exercise and Sport Science*, W. E. Garrett and D. T. Kirkendall, Eds. Philadelphia, PA: Williams & Wilkins, 2000, pp. 661–674.
- [12] W. D. McArdle, F. I. Katch, and V. L. Katch, *Exercise Physiology: Energy, Nutrition & Human Performance*, 6th ed. Philadelphia, PA: Williams & Wilkins, 2007.
- [13] A. T. Johnson, *Biomechanics and Exercise Physiology: Quantitative Modeling*. Boca Raton, FL: CRC, 2007.
- [14] G. Radegran and B. Saltin, "Muscle blood flow at onset of dynamic exercise in humans," *Amer. Physiol. Soc.*, vol. 274, pp. 314–322, 1998.
- [15] T. Kawada, G. Sunagawa, H. Takaki, T. Shishido, H. Miyano, H. Miyashita, T. Sato, M. Sugimachi, and K. Sunagawa, "Development of a servo-controller of heart rate using a treadmill," *Jpn. Circ. J.*, vol. 63, pp. 945–950, 1999.
- [16] R. A. Cooper, T. L. Fletcher-Shaw, and R. N. Robertson, "Model reference adaptive control of heart rate during wheelchair ergometry," *IEEE Trans. Control Syst. Technol.*, vol. CST-6, no. 4, pp. 507–514, Jul. 1998.
- [17] A. S. Matveev and A. V. Savkin, *Qualitative Theory of Hybrid Dynamical Systems*. Boston, MA: Birkhäuser, 2000.
- [18] A. V. Savkin and R. J. Evans, *Hybrid Dynamical Systems. Controller and Sensor Switching Problems*. Boston, MA: Birkhäuser, 2002.
- [19] F. Dela, T. Mohr, C. M. R. Jensen, H. L. Haahr, N. H. Secher, F. Biering-Sørensen, and M. Kjær, "Cardiovascular control during exercise: Insight from spinal cord-injured humans," *Circulation*, vol. 107, pp. 2127–2133, 2003.
- [20] Y. Bard, *Nonlinear Parameter Estimation*. New York/London, U.K.: Academic, 1974.
- [21] W. J. H. Stortelder, "Parameter estimation in dynamic systems," *Math. Comput. Simul.*, vol. 42, pp. 135–142, 1996.
- [22] P. L. Bonate, *Pharmacokinetic-Pharmacodynamic Modeling and Simulation*. New York: Springer-Verlag, 2006.
- [23] G. A. F. Seber and C. J. Wild, *Nonlinear Regression*. New York: Wiley, 1989.
- [24] I. R. Petersen, V. A. Ugrinovskii, and A. V. Savkin, *Robust Control Design Using  $H^\infty$  Methods*. London, U.K.: Springer-Verlag, 2000.
- [25] A. Rantzer and M. Johansson, "Piecewise linear quadratic optimal control," *IEEE Trans. Autom. Control*, vol. AC-45, no. 4, pp. 629–637, Apr. 2000.
- [26] S. Hedlund and M. Johansson, "PWLTool, a MATLAB toolbox for piecewise linear system," Dept. Autom. Control, Lund Inst. Technol., Lund, Sweden, Tech. Rep. ISRN LUTFD2/TFRT-7582-SE, 1999.
- [27] S. Skogestad and I. Postlethwaite, *Multivariable Feedback Control*. Chichester, U.K.: Wiley, 1996.
- [28] P. J. Diggle, *Time Series: A Biostatistical Introduction*. Oxford, U.K.: Oxford Univ. Press, 1990.



**Teddy M. Cheng** (S'95–M'05) received the B.E. degree in aeronautical engineering from the University of Sydney, Sydney, NSW, Australia, in 1995, the M.E. degree in electrical engineering from Queensland University of Technology (QUT), Brisbane, Qld., Australia, in 1998, and the Ph.D. degree in electrical engineering from The University of New South Wales (UNSW), Sydney, in 2004.

Since 2004, he has been a Postdoctoral Researcher with the School of Electrical Engineering and Telecommunications, UNSW. His current research interests include networked control systems, nonlinear and robust control, and modeling and control of biomedical systems.



**Andrey V. Savkin** (M'97–SM'98) was born in 1965 in Norilsk, Russia. He received the M.S. degree in mathematics and the Ph.D. degree in applied mathematics from The Leningrad University, Leningrad, Russia, in 1987 and 1991, respectively.

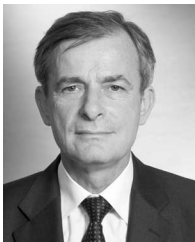
From 1987 to 1992, he was with the All-Union Television Research Institute, Leningrad. From 1992 to 1994, he was a Postdoctoral Fellow in the Department of Electrical Engineering, Australian Defence Force Academy, Canberra. From 1994 to 1996, he was a Research Fellow in the Department of Electrical and Electronic Engineering and the Cooperative Research Center for Sensor Signal and Information Processing, University of Melbourne, Melbourne, Vic., Australia. In 1996, he joined the Department of Electrical and Electronic Engineering, The University of Western Australia, Perth, Australia, as a Senior Lecturer, where he later became an Associate Professor. Since 2000, he has been a Professor in the School of Electrical Engineering and Telecommunications, The University of New South Wales, Sydney, NSW, Australia. His current research interests include robust control and filtering, hybrid dynamical systems, networked control systems, computer-integrated manufacturing, control of mobile robots, computer vision, and application of control and signal processing to biomedical engineering and medicine. He has authored or coauthored four books and numerous journal and conference papers.

Dr. Savkin has been an Associate Editor for several international journals and conferences.



**Steven W. Su** (M'99) received the B.S. and M.S. degrees from Harbin Institute of Technology (HIT), Harbin, China, in 1990 and 1993, respectively, and the Ph.D. degree from the Research School of Information Sciences and Engineering (RSISE), The Australian National University (ANU), Canberra, A.C.T., Australia, in 2002.

From 2002 to 2004, he was a Postdoctoral Research Fellow in the School of Chemical Engineering and Industrial Chemistry, The University of New South Wales (UNSW), Sydney, NSW, Australia, where he was a Visiting Lecturer at the Biomedical System Laboratory, School of Electrical Engineering, and from 2004 to 2006, a Research Fellow in the School of Electrical Engineering and Telecommunications. He is currently a Lecturer in the Group of Mechatronics and Intelligent Systems, Faculty of Engineering, University of Technology Sydney (UTS), Sydney. His current research interests include biomedical system modeling and control, robust and adaptive control, fault tolerant control, nonlinear process control, and navigation system design.



**Branko G. Celler** (M'88) received the B.Sc. and B.E. (Hons.) degrees in electrical engineering and the Ph.D. degree in biomedical engineering from The University of New South Wales (UNSW), Sydney, NSW, Australia, in 1969, 1971, and 1978, respectively.

He was a Postdoctoral Fellow at the Johns Hopkins School of Medicine, Baltimore, MD. In 1981, he joined the UNSW, where he was the Foundation Director of the Biomedical Systems Laboratory, the Human Performance Laboratory, and the Centre for Health Informatics, and the Head of the School of Electrical Engineering and Telecommunications, for almost nine years. He is currently the Chief Executive Officer of TeleMedCare Pty. Ltd., Rosebery, NSW, and the Director of the Biomedical Systems Laboratory, UNSW. His current research interests include biomedical instrumentation and systems, noninvasive modeling of cardiovascular performance, home telecare and remote monitoring, and medical informatics.



**Lu Wang** received the M.E. degree in computer science and the Ph.D. degree in electrical engineering from The University of New South Wales (UNSW), Sydney, NSW, Australia, in 2002 and 2006, respectively.

She was a Research Associate in the School of Electrical Engineering and Telecommunications, UNSW. She is currently an Electrical Engineer at Cochlear Ltd., Lane Cove, NSW. Her current research interests include mathematical modeling of human cardiovascular and respiratory system, exercise physiology, and analysis of cardiovascular and respiratory variability signals.